

## The formation and differentiation of magmas

Persikov E.S.<sup>1</sup>, Bukhtiyarov P.G.<sup>1</sup>, Aranovich L.Ya.<sup>1,2</sup>, Nekrasov A.N.<sup>1</sup>, Kosova C.A.<sup>1</sup> **Metal-silicate separation in andesite melts interacting with hydrogen (experimental study).**

<sup>1</sup> IEM RAS, <sup>2</sup> IGEM RAS [persikov@iem.ac.ru](mailto:persikov@iem.ac.ru)

**Abstract.** It has been established that, despite the high reduction potential of the system  $H_2$  - andesite melt, the reactions of hydrogen oxidation and reduction of Fe oxides in the melt do not go to the end. Initially, homogeneous andesite melts become heterogeneous.  $H_2O$  is formed in the fluid phase (originally pure hydrogen);  $H_2O$  (0.1 – 0.5 wt.%) dissolves in andesite melts, and small metallic droplets of liquification texture are formed in them at a temperature significantly lower than the melting point of the metal. In our experiments, metal droplets are formed at temperatures below the melting point of iron ( $\sim 300$  °C) at atmospheric pressure. The process of forming a liquid-like structure Fe (mainly small spheres of several microns) due to redox reactions is undoubtedly complex.

**Keywords:** andesite, hydrogen, pressure, high temperature, interaction

The first experimental data on the interaction of andesite melts with hydrogen at a temperature of 1250 °C, a hydrogen pressure of 100 MPa under reducing conditions ( $f(O_2) = 10^{-13} - 10^{-14}$ ) were obtained. The experiments were conducted using the original high-gas pressure installation. The installation includes a gas (Ar) compression system that creates pressure in a high-pressure gas vessel with internal heating. Inside this vessel, a unique device is installed, which for the first time provides for long-term experiments at high temperatures and pressures of hydrogen (Fig. 1).

The experiments used natural samples of andesite of the volcano Avacha (Kamchatka). After bringing the installation into the experimental mode for temperature and pressure of hydrogen, an exposure of 5 hours was carried out at these parameters, and then a quick ( $\sim 300$  °C / min) isobaric quenching was carried out. On the basis of experiments, the following features of the process of interaction of hydrogen with andesite melt have been established. As previously established in the basalt-hydrogen system (Persikov et al., 1990; Persikov et al., 2019, 2019a), in the andesite melt-hydrogen system, also initially homogeneous melts become heterogeneous.  $H_2O$  is formed in the fluid phase (originally pure hydrogen);  $H_2O$  (0.1 – 0.5 wt.%) dissolves in andesite melts, and small metallic droplets of liquation texture are formed in them at a temperature significantly lower than the melting point of metals. In our experiments, metal droplets are formed at temperatures below the melting point of iron ( $\sim 300$  °C) at atmospheric pressure.

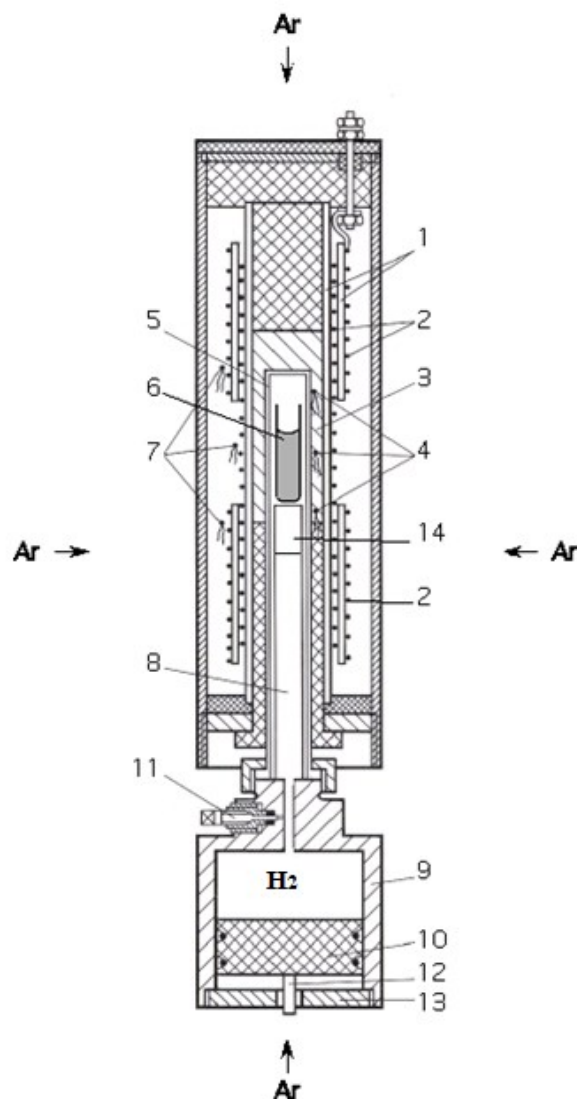
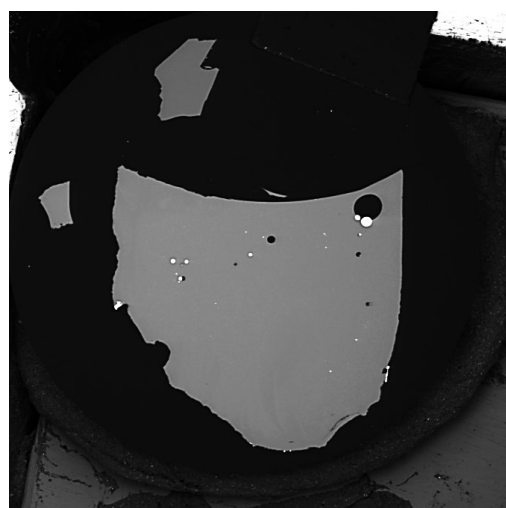


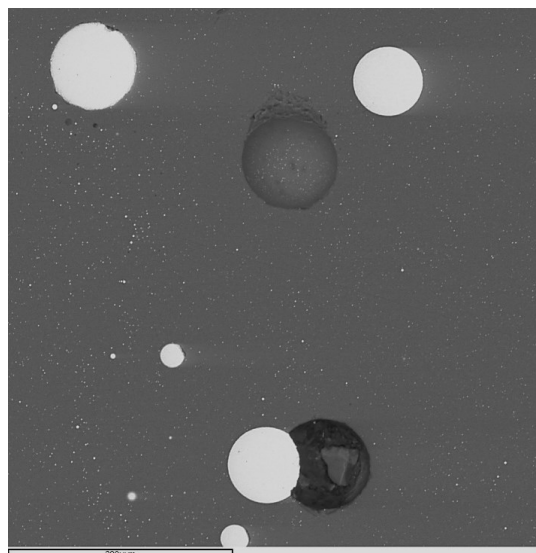
**Fig. 1.** Scheme of the unique internal device and internal heater of the high-pressure vessel. 1, 3 - insulators; 2 - two heater windings; 4 - three thermocouples to control the temperature gradient along the ampoule with the sample; 5 - molybdenum tube; 6 - molybdenum ampoule with a sample of andesite; 7 - two thermocouples to control the temperature of each heater winding; 8 - sapphire cylinder; 9 - equalizer -separator vessel; 10 - equalizer-separator piston; 11 - valves; 12 - sensor for monitoring the position of the piston; 13 - cover; 14 - ampoule with oxygen buffer.

The process of formation of the liquid-like structure of Fe (mainly small ideal spheres with a diameter of up to 100 microns, (Fig. 2b) due to redox reactions is undoubtedly complex. Note that the structure and size of the experimentally obtained metal droplets are well consistent with natural data on the findings of small amounts of the metallic phase, primarily iron in igneous rocks of various composition and genesis under the conditions of the earth's crust (Oleynikov, 1985; Ryabov et al., 1985).



SEM HV: 20.00 kV  
SEM MAG: 40 x  
Nekrasov A.M.  
Vac: HVVac  
View field: 9.54 mm  
Det: BSE-Detector + SE-Detector

(a)



(b)

**Fig. 2.** The result of the experiment on the interaction of andesite melt with hydrogen. Raster microphotography in reflected electrons of the quench sample; (a) is the cross-section of the sample after the experiment is an andesite melt (glass) with small balls of metallic phase and a slightly more acidic composition (Table 1); (b) – balls of metallic phase found in andesite melt (dark color - silicate glass, composition see Table 1), white color - metallic phase, composition see Table 2).

**Table 1.** Chemical compositions (wt. %) and structural-chemical parameter (100NBO/T) of initial andesite glasses and melts (glass) after experiments under hydrogen pressure

Components	№ 2156	Initial andesite glass, volcano Avacha (Kamchatka)
SiO <sub>2</sub>	60.77	58.8
Al <sub>2</sub> O <sub>3</sub>	16.69	16.62
Fe <sub>2</sub> O <sub>3</sub>	0.00	1.0
FeO	3.33	5.66
MnO	0.1	0.11
MgO	5.58	5.59
CaO	7.0	6.77
Na <sub>2</sub> O	4.28	4.18
K <sub>2</sub> O	1.38	1.32
TiO <sub>2</sub>	0.66	0.59
P <sub>2</sub> O <sub>5</sub>	0.09	0.20
H <sub>2</sub> O-	0.2	0.11
Sum	100.08	100.95
100NBO/T	35.6	39.1

*Note:*  
The average values from the analysis of 23 points of each sample are given.

**Table 2.** Chemical compositions (wt. %) of metallic phases in andesite melts (glass) after experiments under hydrogen pressure

Components	№ 2156
Fe	97.25
Mg	0.03
Ti	0.1
O	0.6
Si	0.04
Ca	0.15
P	1.2
Sum	99.37

*Note:*  
1. The results presented in the table are the average values of 7 dimensions.  
2. The concentrations of all impurity elements (Si, Ca, Ti, Mg) in the metallic phases are determined approximately, since these values are within the limits of analytical errors.

*Sources of funding: RSF, grant No. 22-27-00124 partially state assignment under the theme No FMUF-2022-0004 IEM RAS*

#### References

1. Native metals in igneous rocks (1985) All-Union conference. Abstracts, part 1. Ed. B. V. Oleynikov).

- Yakutsk: YB of USSR Acad. Sci. 188 p. (in Russian).
- Persikov E.S., Zharikov V.A., Bukhtiyarov P.G., Pol'skoy S.F. (1990) The effect of volatiles on the properties of magmatic melts. *Eur. J. Mineral.*, **2**, 621- 642.
  - E.S. Persikov, P.G. Bukhtiyarov, L.Ya. Aranovich A.N., Nekrasov, O.Yu. Shaposhnikova (2019) Experimental modeling of formation of native metals (Fe,Ni,Co) in the earth's crust by the interaction of hydrogen with basaltic melts. *Geochemistry International*, **57**, No. 10, p. 1035–1044.
  - Persikov E. S., Bukhtiyarov P. G., Aranovich L. Ya., Shchekleina M.D. (2019a). Features of hydrogen interaction with basaltic melts at pressures 10 - 100 MPa and temperatures 1100 - 1250 °C. Programme and Abstracts. 11-th Silicate Melt Workshop. La petite Pierre, France. 1-5 October, p. 64.
  - Ryabov V. V., Pavlov A. L., Lopatin G. G. (1985) Native iron in Siberian traps. Novosibirsk: Nauka SB RAS, 167 p. (in Russian).

**Persikov E.S.<sup>1</sup>, Bukhtiyarov P.G.<sup>1</sup>, Aranovich L.Ya.<sup>1,2</sup>, Bondarenko G.V.<sup>1</sup> Some features of the interaction of iron with methane at a temperature of 900 °C and a pressure of 100 MPa.**

<sup>1</sup>IEM RAS, Chernogolovka, <sup>2</sup>IGEM RAS, Moscow  
[persikov@iem.ac.ru](mailto:persikov@iem.ac.ru)

**Abstract.** Using the original high-gas pressure unit, experiments were performed for the first time on the interaction of iron with methane at a temperature of 900 °C and a pressure of 100 MPa. Note that the experimental data on the possibility of the joint entry of hydrogen and carbon into metallic iron at high pressures are contradictory. Complex methods (microprobe, Raman spectroscopy, mass balance calculations) are used for a thorough analysis of the composition of the metal phases formed in hardening experiments. Unlike the previously studied Fe<sub>3</sub>C-H<sub>2</sub> system, when Fe reacts with methane, there is an active interaction of carbon with iron up to the synthesis of Fe<sub>3</sub>C carbide.

**Keywords:** iron, methane, pressure, high temperature, interaction

The role of hydrogen, the most abundant element of our Galaxy, in natural processes is extremely diverse and in recent years has attracted increasing attention of petrologists and geochemists. Including the important problem of the joint entry of hydrogen and carbon into metallic iron at high and ultra-high pressures remains debatable (Morard et al., 2017; Fei, Brosh, 2014); Narygina et al., 2011; Litasov et al., 2016; et al.). The proposed work presents the first results of experiments on the interaction of Fe with methane in open sapphire and molybdenum ampoules at a pressure of 100 MPa created by pure CH<sub>4</sub>, a temperature of 900 °C and an experiment duration of 24 hours. The experiments were carried out at a unique high-gas pressure install. This install

is equipped with an original internal device (Fig. 1), which made it possible to conduct long-term experiments at such high temperatures, despite the high penetrating power of hydrogen formed in the experiments due to the pyrolysis of methane (Persikov et al., 2020). The internal volumes of the molybdenum reactor (5) with open sapphire and molybdenum ampoules with starting samples Fe, approximately 200 mg (6) each and a separator equalizer (9) under the piston (10), were filled with methane at a pressure of 10 MPa using a special system. The device assembled in this way, together with the internal heater (2), was placed inside the high-pressure vessel so that the ampoules with the samples (6) were in the gradient-free temperature zone of the heater. Due to the movement of the piston (10), the gas (Ar) pressure in the vessel during the experiment was always maintained equal to the methane pressure in the internal volume of the reactor (5). At the beginning of the experiment, the pressure of argon in the vessel and, accordingly, methane in the reactor (5) was raised within one hour to the required value of 100 MPa. Next, the temperature of the experiment was raised to the required value of 900 °C. At these parameters, the samples were kept in automatic mode for the required time of experiments (24 hours), after which isobaric hardening was carried out with the internal heater of the installation turned off. At the same time, a sufficiently high hardening speed of the sample was achieved (~ 300 °C / min). The error of measuring the temperature of the experiment was ± 5 °C, and the methane pressure ± 0.1% RH. After isobaric hardening, pressure relief in the vessel and complete cooling, the internal device was removed from the high-gas pressure vessel, ampoules with samples were extracted from the molybdenum reactor for subsequent analysis of the phases formed during the experiment. The device assembled in this way, together with the internal heater (2), was placed inside the high-pressure vessel so that the ampoules with the samples (6) were in the gradient-free temperature zone of the heater. By moving the piston (10), the pressure of methane in the internal volume of the reactor (5) was always kept equal to the pressure of the gas (Ar) in the vessel during the experiment. At the beginning of the experiment, the pressure of argon in the vessel and, accordingly, methane in the reactor (5) was raised within one hour to the required value of 100 MPa. Next, the temperature of the experiment was raised to the required value of 900 °C. At these parameters, the samples were kept in automatic mode for the required time of experiments (24 hours), after which isobaric hardening was carried out with the internal heater of the installation turned off. At the same time, a sufficiently high hardening speed of the sample was achieved (~ 300 °C / min). The error of measuring

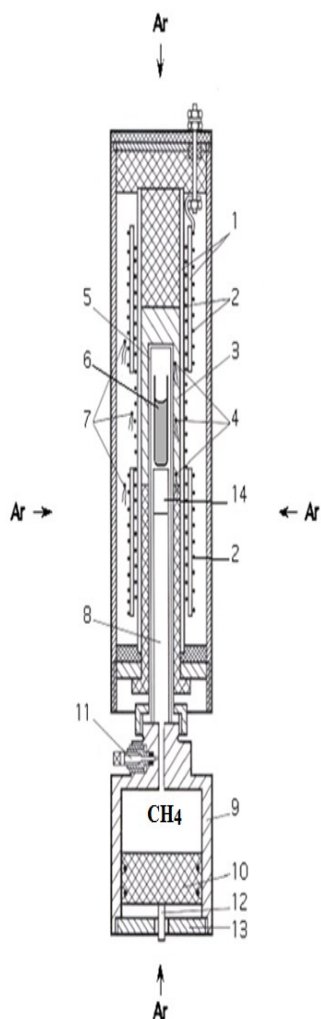


**Fig. 1.** Scheme of the unique internal device and internal heater of the high-pressure vessel. 1, 3 - insulators; 2 - two heater windings; 4 - three thermocouples to control the temperature gradient along the ampoules with samples; 5 - molybdenum tube; 6 - molybdenum and sapphire ampoules with Fe samples; 7 - two thermocouples to control the temperature of each heater winding; 8 - sapphire cylinder; 9 - separator-separator vessel; 10 - equalizer-separator piston; 11 - valves; 12 - sensor for monitoring the position of the piston; 13 - cover; 14 - ampoule with oxygen buffer

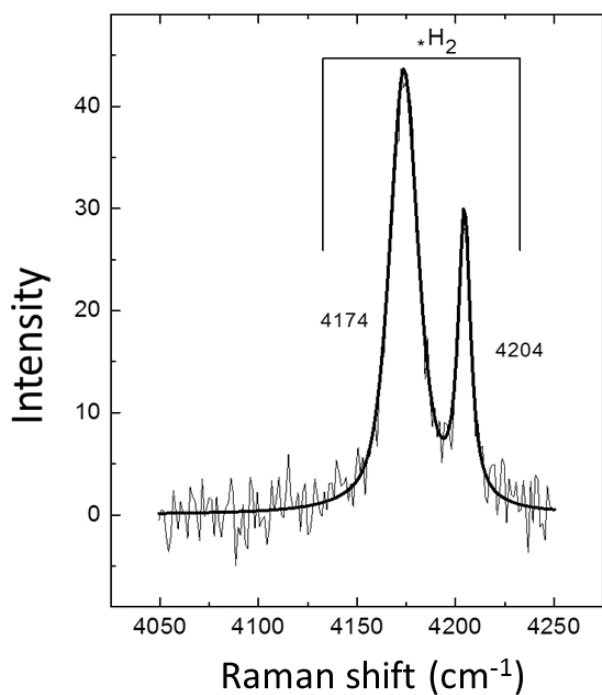


**Fig. 2.** Raman scattering spectrum of the sample (experiment No 2153 in the field of valence oscillation of hydrogen (Persikov et al., 2020; Idalou et al., 2019))

the temperature of the experiment was  $\pm 5^\circ \text{C}$ , and the methane pressure  $\pm 0.1\% \text{RH}$ . After isobaric

hardening, pressure relief in the vessel and complete cooling, the internal device was removed from the

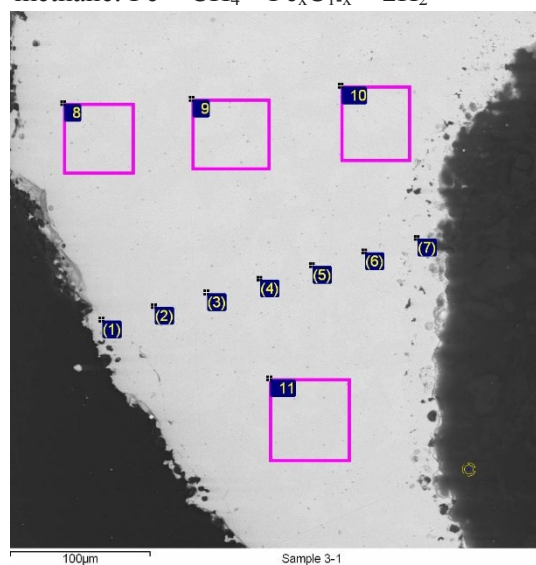
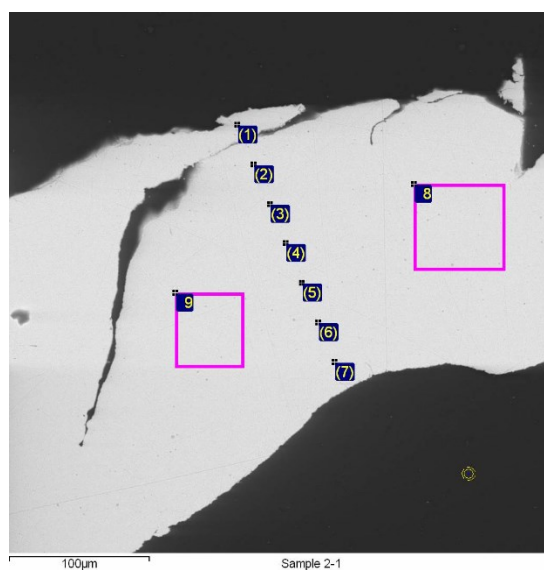
high-gas pressure vessel, ampoules with samples were extracted from the molybdenum reactor for subsequent analysis of the phases formed during the experiment. Pieces of pure iron Fe were used as the starting sample. Chemical compositions of initial Fe samples and phases obtained in the experiments (Fig. 3), determined using a digital electron X-ray microscope CamScan MV2300 (VEGA TS 5130 MM), with a prefix for energy-dispersion microanalysis INCA Energy 450 and WDS Oxford INCA Wave 700. Analyzes were carried out at an accelerating voltage of 20 kV with a beam current of up to 400 nA and a spectral set time of 50 -100 seconds.

The carbon content in hardened samples after experiments (see table, Fig. 3) was determined by the difference between the sums of the analyzed elements and the stoichiometric one. This C content in the samples was further controlled by analyzing the results of the mass balance of experience. Qualitative confirmation of the presence of hydrogen in hardened sample No. 2153 was performed using Raman spectroscopy (Fig. 2). Raman spectra were obtained using the *RM1000* spectrometer

(Renishaw), equipped with a CCD camera, a boundary filter and a *Leica DMLM* microscope.

Unlike the previously studied Fe<sub>3</sub>C-H<sub>2</sub> system, when Fe reacts with methane, the carbon formed after the pyrolysis of methane reacts actively with iron up to the synthesis of Fe<sub>3</sub>C carbide in a molybdenum ampoule on the surface of the sample (Fig. 3). Evidence of the mentioned pyrolysis of methane at the parameters of the experiment was a large amount of soot found in ampoules with samples after the experiments. Such a significant degree of pyrolysis of methane in the experiments is probably associated with the catalytic effect of the Fe samples themselves, as well as the reactor material and ampoules, to a greater extent Mo, and less sapphire. Figure 3 presents the results of a microprobe analysis of the carbon distribution in the samples after experiment 2153. These results indicate an active interaction of carbon with Fe on the surface of the samples with the formation of Fe<sub>3</sub>C carbide in the molybdenum ampoule (Fig. 3b) and the diffusion distribution of C in the depth of the samples in both ampoules.

Reaction controlling the interaction of Fe with methane:  $Fe + CH_4 = Fe_xC_{1-x} + 2H_2$  (1)



Spectra	Fe	C	Spectra	Fe	C
1	87.55	12.45	1	76,49	23,51
2	89.08	10.92	2	74,61	25,39
3	86.64	13.36	3	74,81	25,19
4	85.36	14.64	4	88,47	11,53
5	88.14	11.86	5	85,1	14,9
6	86.75	13.25	6	66,67	33,33
7	88.0	12.0	7	65,1	34,9
8	87.5	12.5	8	85,86	14,14
9	98.9	1.1	9	86,03	13,97
			10	76,55	23,45
			11	82	18

(a)

(b)

**Fig. 3.** Raster micrographs in reflected electrons and C distribution in products of quenching of Fe samples under methane pressure, experiment 2135 (in tables at. %), (a) – sample Fe in sapphire ampoule, (b) – sample Fe in molybdenum ampoule

Sources of funding: RSF, grant No. 22-27-00124 partially state assignment under the theme No FMUF-2022-0004 IEM RAS

## References

1. Idalou C., Hirschmann, M.M. Jacobsen, S.D. Le Losq C. (2019). Raman spectroscopy study of C-O-H-N speciation in reduced basaltic glasses: Implications for reduced planetary mantles. *Geochimica et Cosmochimica Acta*, **265**, 32-47.
2. Litasov K.D., Shatskiy A.F., Ohtani E. (2016). Interaction of Fe and Fe<sub>3</sub>C with Hydrogen and Nitrogen at 6–20 GPa: a Study by in Situ X-Ray Diffraction. *Geochem. Inter.*, **54**, 914–921
3. Fei Y., Brosh E. (2014). Experimental study and thermodynamic calculations of phase relations in the Fe–C system at high pressure. *Earth and Planetary Science Letters*, **408**, 155–162.
4. Morard G., Andraut D., Antonangeli D., et al. (2017). Fe–FeO and Fe–Fe<sub>3</sub>C melting relations at Earth's core–mantle boundary conditions: Implications for a volatile-rich or oxygen-rich core. *Earth and Planetary Science Letters*, **473**, 94–103.
5. Narygina, O., Dubrovinsky, L. S., McCammon, C. A., et al. (2011). X-ray diffraction and Meossbauer spectroscopy study of fcc iron hydride FeH at high pressures and implications for the composition of the Earth's core. *Earth and Planetary Science Letters*, **307**, 409–414.
6. Persikov E. S., Bukhtiyarov P. G., Aranovich L. Ya., Shchekleina M.D. (2020). Features of hydrogen interaction with basaltic melts at pressures 10 - 100 MPa and temperatures 1100 – 1250 °C. *Chemical Geol.*, **556**, p. 5 December.

## Persikov E.S.<sup>1</sup>, Bukhtiyarov P. G.<sup>1</sup>, Aranovich L.Ya.<sup>1,2</sup>, Shaposhnikova O.Yu.<sup>1</sup> Features of the process of interaction of hydrogen with andesite-basalt melts in conditions of dynamic mode.

<sup>1</sup>IEM RAS, <sup>2</sup>IGM RAS persikov@iem.ac.ru

**Abstract.** New experimental data on the interaction of igneous melts with hydrogen in a dynamic mode at a temperature of 1200 °C and hydrogen pressures (75 - 100 MPa) were obtained, which make it possible to understand the possible role of hydrogen in the processes occurring in magma in the earth's crust and the volcanic process under reducing conditions ( $f(O_2) = 10^{-13} - 10^{-14}$ ). Natural samples of igneous rocks were used in the experiments: the magnesian basalt of the Northern breakthrough of the Tolbachik volcano (Kamchatka), and the andesite of the Avacha volcano (Kamchatka). On the basis of experiments, it has been shown that all the features of the interaction of hydrogen with basalt melts, established earlier in static experiments, are preserved, but at the same time the intensity of the release of the metallic phase and the degree of acidification of the original andesite and basalt melts are significantly increased.

**Keywords:** basalt, andesite, melt, hydrogen, pressure, high temperature, interaction

In continuation of our early research (Persikov et al., 1990), new experimental data were obtained on the interaction of igneous melts with hydrogen at a temperature of 1200 °C and hydrogen pressures (75 - 100 MPa) under dynamic conditions, allowing us to understand the possible role of hydrogen in the processes occurring in magma in the earth's crust and the volcanic process under reducing conditions ( $f(O_2) = 10^{-13} - 10^{-14}$ ). The experiments were conducted using the original high-gas pressure installation. The installation includes a gas (Ar) compression system that creates pressure in a high-pressure gas vessel with internal heating. Inside this vessel, a unique device is installed, which for the first time provides for long-term experiments at high temperatures and pressures of hydrogen (Fig. 1).

The dynamic mode of one of the experiments (No. 2105) is given in the caption to Table 1. Natural samples of igneous rocks were used in the experiments: magnesian basalt of the northern breakthrough of the Tolbachik volcano (Kamchatka) and the andesite of the Avacha volcano, Kamchatka (Table 1). On the basis of experiments, the following features of the process of interaction of hydrogen with igneous melts in a dynamic mode have been established:

1. Despite the high reduction potential of the H<sub>2</sub> - magmatic melt system, the reactions of hydrogen oxidation and complete reduction of metal oxides of variable valence in the melt do not go to the end.

2. Initially homogeneous igneous melt becomes heterogeneous: the formed H<sub>2</sub>O dissolves in the melt and in the fluidic phase (initially pure hydrogen); all the features of the interaction of hydrogen with basalt melts, established earlier in static experiments [Persikov et al., 2019, 2019a], are preserved, but at the same time the intensity of the release of the metallic phase of the liquation structure (Fig. 2, 3; the composition see Table 2) and the degree of acidification of the initial andesite and basalt melts (Table 1) are significantly increased.

3. A complex process of metal-silicate liquification in magmatic melts when they interact with hydrogen can be carried out at real magma temperatures in nature ( $\leq 1200$  °C), significantly lower than the corresponding melting points of iron (1560 °C) (Fig. 2a).

4. The structure and size of the experimentally established metal partitions agree well with natural data on the findings of small amounts of native metals, primarily iron and its alloys with nickel and cobalt, in igneous rocks of different composition and genesis (Persikov et al., 2019, 2019a; Ryabov et al., 1985).

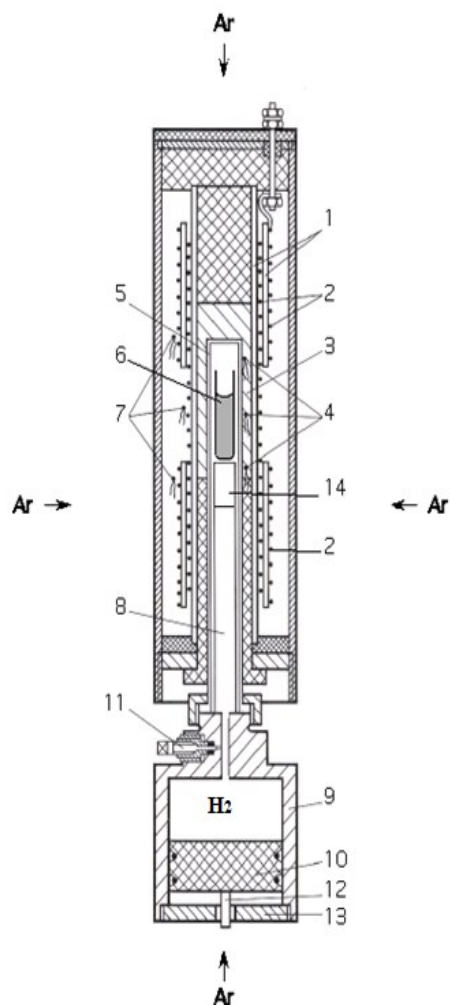


**Fig. 1.** Scheme of the unique internal device and internal heater of the high-pressure vessel. 1, 3 - insulators; 2 - two heater windings; 4 - three thermocouples to control the temperature gradient along the Pt ampoule with the sample; 5 - molybdenum tube; 6 - platinum ampoule with a combined sample (basalt in the lower half of the sample and andesite in the upper); 7 - two thermocouples to control the temperature of each heater winding; 8 - sapphire cylinder; 9 - equalizer-separator vessel; 10 - equalizer-separator piston; 11 - valves; 12 - sensor for monitoring the position of the piston, 13 - cover; 14 ampoule with oxygen buffer

**Table 1.** Chemical composition (wt. %) and structural-chemical parameter (100NBO/T) of initial rocks, minerals and melts (glass) after experiments under hydrogen pressure under dynamic conditions

Com- ponents	№ 2105				Magnesian basalt, initial composition	Andesite, initial composition
	*	**	***	****	*****	*****
SiO <sub>2</sub>	56.22	67.48	39.2	55.55	49.5	58.8
Al <sub>2</sub> O <sub>3</sub>	15.41	17.57	0.26	27.86	13.18	16.62
Fe <sub>2</sub> O <sub>3</sub>	0.00	0.00	no	0.0	3.18	1.0
FeO	0.86	1.96	13.0	0.5	6.85	5.66
MnO	0.2	0.1	no	no	0.15	0.11
MgO	9.44	1.27	46.43	0.1	9.98	5.59
CaO	12.7	5.48	0.05	10.65	12.34	6.77
Na <sub>2</sub> O	2.63	4.55	0.06	4.96	2.18	4.18
K <sub>2</sub> O	0.95	1.08	0.06	0.1	0.93	1.32
TiO <sub>2</sub>	0.85	0.34	0.01	0.0	1.01	0.59
P <sub>2</sub> O <sub>5</sub>	0.20	0,21	no	no	0.25	0.2
H <sub>2</sub> O-	0	0	0.0	no	0.29	0.11
Sum	100	100	100	100	99.84	100.95
100NBO/T	62.5	9.2	400	1.0	83	39.1

*Notes:*

\* glass in the zone of the original magnesian basalt: P (H<sub>2</sub>) = 100 MPa, T = 1200 °C, holding 1 hour, then reducing the hydrogen pressure to 75 MPa in isothermal mode for 1 hour (purging), holding 1 hour, and then isobaric quenching.

\*\* glass in the area of the original andesite;

\*\*\*olivines in the zone of magnesia basalt;

\*\*\*\* plagioclases in the zone of the original andesite;

\*\*\*\*\* magnesian basalt of the northern breakthrough of the Tolbachik volcano, eruption 1975-1976, Kamchatka

\*\*\*\*\* andesite from volcano Avacha, Kamchatka (Persikov et al., 1990).

**Table 2.** Chemical compositions (wt. %) of metallic phases in basalt and andesite melts (quenched samples) after dynamic experiments under hydrogen pressure

Components	№ 2105	№ 2105
	*	**
Fe	98.1	98.07
Mg	0.08	0.84
Ti	0.04	0.08
O	0.58	1.2
Si	0.02	0.16
Ca	0.19	0.23
P	0.98	0.52
Sum	100.8	101.1

*Notes:*

\* - metallic phase in the zone of the original magnesian basalt.

\*\* - metallic phase in the zone of the original andesite.

1. The results presented in the table are the average values of 7 dimensions.

2. The concentrations of all impurity elements (Si, Ca, Ti) in the metallic phases are determined approximately, since these values are within the limits of analytical errors.

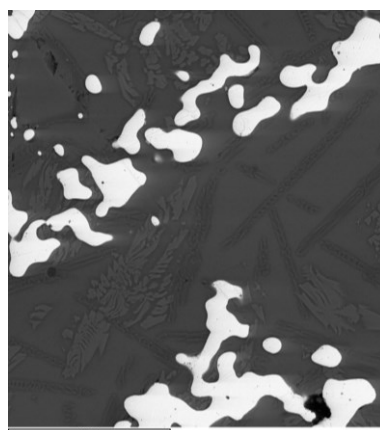
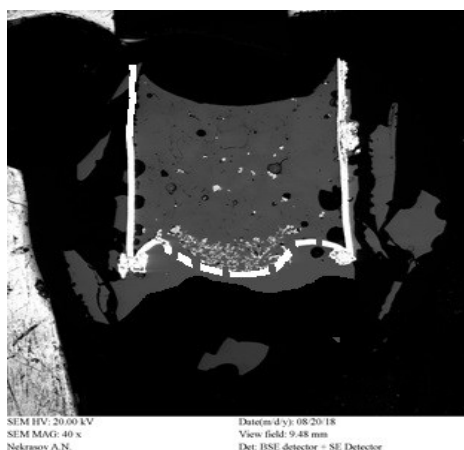


**Fig. 2.** The result of dynamic experience on the interaction of andesite - basalt melt with hydrogen. Raster microphotography in reflected electrons of the hardening sample;

(a) - the cross-section of the sample after a dynamic experiment: the lower half of the sample is originally a basalt melt with a large amount of isolated metallic phase at the bottom formed in the experiment; the upper half of the sample is originally an andesite melt with small balls of metallic phase and a much more acidic composition (Table 1);  
 (b) – metallic secretions found in the initial basalt half of the sample (dark - silicate glass, white - metallic phase, composition of the metal phase see Table 2).

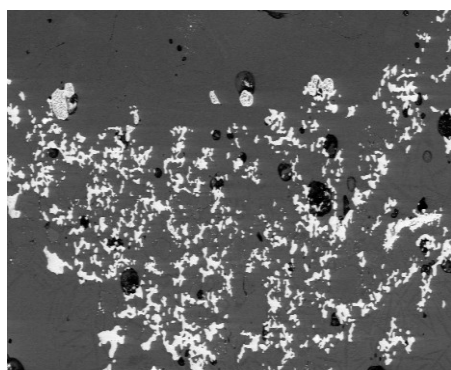


**Fig. 3.** Comparison of the structure of experimental and natural samples

(a) - Raster microphotography in reflected electrons of sample quenched products after experiments on the interaction of basalt melt under hydrogen pressure in dynamic mode, experiment 2105 (white color-metallic iron, composition see table 2; black color-basalt glass, composition see table 1)  
 (b) – interspersed ore of native iron in the gabbro-dolerite of the intrusion of Mount Ozernaya (white color-native iron, black color - gabbro-dolerite, full size, Ryabov et al, 1985)

Sources of funding: RSF, grant No. 22-27-00124 partially state assignment under the theme No FMUF-2022-0004 IEM RAS

**References**

1. Persikov E.S., Zharikov V.A., Bukhtiyarov P.G., Pol'skoy S.F. (1990) The effect of volatiles on the properties of magmatic melts. *Eur. J. Mineral.*, **2**, p. 621- 642.
2. E.S. Persikov, P.G. Bukhtiyarov, L.Ya. Aranovich, A.N., Nekrasov, O.Yu. Shaposhnikova (2019) Experimental modeling of formation of native metals (Fe,Ni,Co) in the earth's crust by the interaction of

- hydrogen with basaltic melts. *Geochemistry International*, **57**, No. 10, p. 1035–1044.
- Persikov E. S., Bukhtiyarov P. G., Aranovich L. Ya., Shchekleina M.D. (2019a). Features of hydrogen interaction with basaltic melts at pressures 10 - 100 MPa and temperatures 1100 - 1250 °C. Programme and Abstracts. 11-th Silicate Melt Workshop. La petite Pierre, France. 1-5 October, p. 64.
  - Ryabov V. V., Pavlov A. L., Lopatin G. G. (1985) Native iron in Siberian traps. Novosibirsk: Nauka SB RAS, 167 p. (in Russian)

**Rusak A.A., Lukanin O.A. Experimental study of silicate melts of basalt composition and the SiO<sub>2</sub>-MgO-FeO-C model system in equilibrium with a liquid iron alloy at high pressures. UDC: 550.4, 552**

Vernadsky Institute of Geochemistry and analytical chemistry RAS (GEOKHI RAS), Russia, 119991, Moscow, st. Kosygina, 19. (aleks7975@yandex.ru; lukanin@geokhi.ru)

**Abstract.** The processes of formation in systems of ultrabasite, basite composition of the metallic phase of iron, which in natural conditions are realized in some basaltic magmas (for example, basalts of the Disco island), and can also occur during the melting of the restored mantle of the Earth and other planetary bodies, were modeled. The formation of liquid metal globules, mainly of Fe-(Ni) composition, was observed in experiments conducted with basite melts at T = 1400 and 1550°C, P = 1,5 and 4 GPa and oxygen volatiles at 1,4 – 1,9 and 0,5 – 2,9 log. units below the Fe-FeO buffer in the presence of graphite. In addition, experiments were carried out in the SiO<sub>2</sub>-MgO-FeO-C system at 1500 – 1600°C and 2.5-3 GPa on a high-pressure installation with a toroidal seal of the "anvil with a hole" type. According to the results of the study of quenching samples, no iron droplets were found in the experimental products. At T = 1600°C and P = 2,5 and 3 GPa, the products of the experiments were glass of the basic composition, quartz crystals and pyroxene. At T = 1500°C and P = 3 GPa, glass with graphite inclusions was formed. The volatility of oxygen in the experiments was controlled by a graphite CCO buffer. A three-component fusibility diagram is constructed for the SiO<sub>2</sub>-MgO-FeO

system, which outlines the area of possible separation of metallic iron droplets under ultra-reducing conditions.

**Keywords:** silicate melt; metallic phase of iron; melting; crystallization; reduced mantle; high pressures; oxygen volatility; CCO buffer; reducing conditions.

**Introduction.** Magma is a multicomponent system containing petrogenic, rare and volatile components. The main factors controlling the transport and composition of volatile components from the subsurface to the Earth's surface are the solubility of volatile components in magma and the redox conditions of their mantle source (Kadik et al., 2006). In modern theories of the formation of the early Earth, the composition of gases of the planet's outer shells is associated with the degassing of magmas formed during the global melting of the mantle ("magmatic ocean") in the presence of the metallic phase of iron (Wetherill, 1990; Walter et al., 2000) at low oxygen fugacity values. The source and composition of the early mantle volatiles remains a debatable issue. According to homogeneous accretion, volatiles could have accumulated from the introduced material of carbonaceous chondrites, which are enriched with water, since CI chondrites mainly consist of water-containing silicates (Wanke et al., 1984). According to the views (Javoy, 1995), carbon and hydrogen were in the silicate mantle of the Earth during the entire process of segregation of iron into the core. The presence of volatile components affects the PT conditions, the composition of the formed mantle magmas (early melting products of the Earth) and their differentiation.

The purpose of this study was to analyze the processes of crystallization and differentiation of magmatic melts under reducing conditions, when a metallic phase of iron is formed in equilibrium with the silicate melt and crystals.

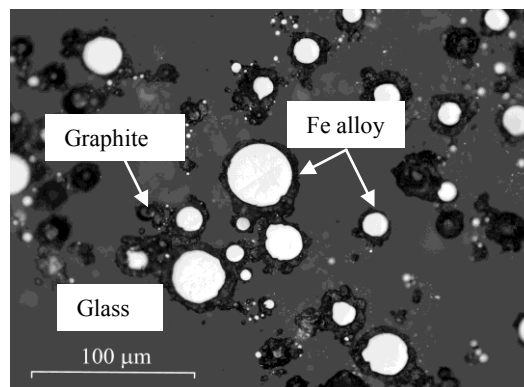
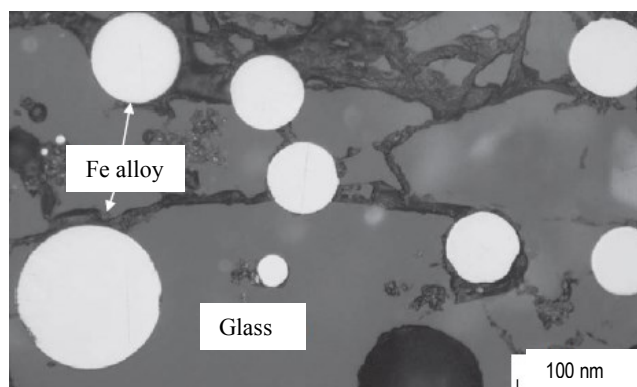


**Fig.1.** Metal drops of iron alloy in glass of basalt composition (images in BSE) (Kadik et al., 2017). Experimental conditions: T = 1400°C, P = 1.5 GPa, ΔlgfO<sub>2</sub>(IW) = -1.8; with the addition of Si<sub>3</sub>N<sub>4</sub> from 0.4 to 2.8 wt. %.

**Fig.2.** Glass with drops of metallic iron (Fe alloy) and graphite crystals (images in BSE) (Lukanin et al., 2020). Experimental conditions: T = 1550°C, P = 4 GPa, ΔlgfO<sub>2</sub>(IW) = -2.9, CSiC = 7 wt. %

## Redox conditions for the formation of the Fe metallic phase in a basalt system containing C-O-H-N volatile components

The formation of liquid metal globules, mainly of Fe-(Ni) composition, was observed in experiments conducted with basalt melts at  $T = 1400^{\circ}\text{C}$ ,  $P = 1.5$  GPa and oxygen volatility by 1.4 – 1.9 log units below the iron-wustite (Fe-FeO) - IW buffer in the presence of an excess of graphite C and nitride silicon ( $\text{Si}_3\text{N}_4$ ) is the source of nitrogen in the system (fig.1) and at  $T = 1550^{\circ}\text{C}$ ,  $P = 4$  GPa and 0.5 – 2.9 log. units below the IW buffer in the presence of graphite and silicon carbide (SiC) are the carbon source in the system (fig. 2).

In the works (Kadik et al., 2017; Lukanin et al., 2020), the forms of dissolution of volatile components were studied and their ratios in basalt melts equilibrium with liquid iron alloy and graphite were estimated by IR and RAMAN spectroscopy of glasses. It is shown that during experiments at  $T = 1400, 1550^{\circ}\text{C}$  and  $P = 1.5; 4$  GPa, nitrogen, hydrogen and carbon are present in the melts in the form of complexes with N-H bonds ( $\text{NH}_3, \text{NH}_4^+$ , etc.), because silicon nitride, N-O (water in molecular form and OH group), C-H ( $\text{CH}_4$ ) and other hydrocarbon complexes, as well as hydrogen and nitrogen molecules. It is also shown that hydrogen dissolves in the melt of the main composition in the form of water and with a decrease in the volatility of oxygen, the concentration of water decreases by half, while the content of methane and other compounds with C-H bonds increases, which indicates the influence of carbon and hydrogen on the restoration of the system. A decrease in  $f\text{O}_2$  leads to the release of the metallic phase and, accordingly, a change in the composition of the melt in terms of silica content from basalt to andesite.

## Experiments on the $\text{SiO}_2\text{-MgO-FeO-C-H}$ system

Tasks of the work are conducting experiments in the  $\text{SiO}_2\text{-MgO-FeO-C-H}$  system at  $T = 1500$  and  $1600^{\circ}\text{C}$  and  $P = 2,5\text{-}3,5$  GPa; construction of a three-component fusibility diagram for the  $\text{SiO}_2\text{-MgO-FeO}$  system.

## Methodology

As an initial mixture, a simplified model gross composition of the Earth ("All Earth") was set according to the data (McDonough, 2017). The initial mixture in terms of the content of the main petrogenic components consisted of powdered quartz ( $\text{SiO}_2$ ) (puriss.spec.), magnesium oxide (MgO) (puriss.spec.) and iron oxalate ( $\text{Fe}_2\text{O}_4$ ), from which  $\text{CO}_2$  was released by heating and FeO (II) remained. A mixture of reagents was melted in quartz ampoules at  $T = 1505^{\circ}\text{C}$  and  $P = 1$  atm in a high-temperature

vertical tubular furnace Nabertherm RHTV 1700 in GEOKHI RAS. The selected pure glass without quartz was placed in the ensemble of a high-pressure installation "anvil with a hole" (NL-13T) with a toroidal seal, and an experiment was conducted at GEOKHI RAS for 40 minutes.

To determine the elemental composition of the solid products of the experiments, the Cameca SX 100 microanalyzer with five wave spectrometers and the Broker Flash 6 energy-dispersion prefix was used at GEOKHI RAS, samples of the Smithsonian Institution's main glass composition (Glass XF2) were used as standards. Micrographs in backscattered electrons (BSE) were obtained at an accelerating voltage of 15 kV and a current of 30 nA. The analytical scanning electron microscope Tescan MIRA 3 at GEOKHI RAS was used to study phase relations and chemical composition. Raster images in BSE were obtained at an accelerating voltage of 20 kV, an operating distance of 15 kV (0,8 nm) and a beam intensity of 14 mA.

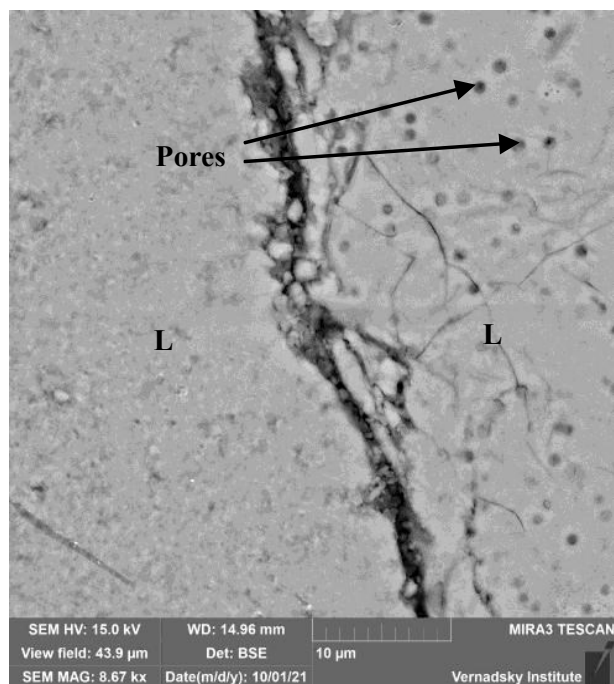
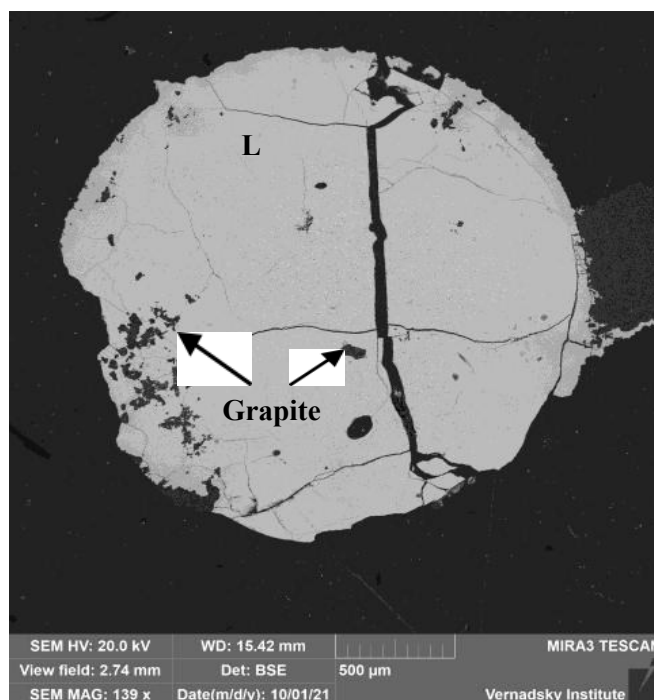
## Results of experiments and discussions

In experiments at a temperature of  $1600^{\circ}\text{C}$  a pressure of 2,5-3 GPa, metal iron droplets were absent, the experimental products were silicate glass of the main composition, quartz up to 25 microns in length and 5-10 microns in width, pyroxene and graphite. The structure of the samples is zonal, glass and quartz in the center, pyroxene on the periphery. Graphite partially penetrated into the edge zone. It occurs as rounded crystals up to 50 microns black in BSE. We work in an "open" system on the "anvil with a hole" installation, the samples are not in a platinum capsule, but in contact with graphite, it is impossible to estimate the gas phase (neither  $\text{CO}$ ,  $\text{CO}_2$ , nor  $\text{CH}_4$ ). The volatility of oxygen in the experiment was controlled by the CCO buffer. When the temperature drops by  $100^{\circ}\text{C}$  and at a pressure of 3 GPa, the structure of the sample changes, it becomes homogeneous. Pyroxene and quartz do not form, a porous glass remains (fig. 3), saturated with CaO, and there are also large graphite crystals, which are mainly located in the marginal zone of the sample, but there are also large crystals in the central part (fig. 4). It is possible that the crystals were captured by the melt during the experiment. There are no metallic iron droplets. At  $1500^{\circ}\text{C}$  CaO migrates to the sample. In order to avoid such problems, in a further experimental study, the assembly of the ensemble will be methodically changed, which will include a sleeve made of MgO:BN in a mass ratio of 3:1 (Bobrov et al., 2011), placed between a graphite heater and a lithographic stone - a toroid. The average compositions of the initial glass and glass after the experiments are presented in Table 1.

**Table 1.** Average compositions of glasses obtained at 1 atm in a tubular furnace, and average compositions of glasses obtained in experiments at  $T = 1600^{\circ}\text{C}$  and  $P = 2,5$  and 3 GPa.

№ exp.	Comp.	SiO <sub>2</sub>	MgO	FeO	Total
The original glass (a)	X (10)	51,36	15,48	33,17	100
	S (10)	2,50	0,91	1,59	
138 (b)	X (4)	52,08	20,40	27,47	100
	S(4)	0,60	1,58	2,14	
159 (c)	X(3)	54,24	16,12	29,64	100
	S(3)	0,14	0,15	0,01	

*Symbols:* a) Average compositions of the original glasses; b) Average compositions of glass in the central zone of the sample (exp.138); c) Average compositions of glass in the central zone of the sample (exp. 159).  $T=1600^{\circ}\text{C}$ ,  $P = 2,5$  and 3 GPa. The data are given in wt. %. X – average values, S – standard deviations. The data indicated in parentheses indicate the number of analyses.

**Fig. 3.** Porous glass ( $T=1500^{\circ}\text{C}$ ,  $P=3\text{GPa}$ , CCO buffer). The image is in BSE.**Fig. 4.** CaO supersaturated glass with large graphite crystals (Grf).

The liquidus surface of the triple fusibility diagram for the SiO<sub>2</sub>-MgO-FeO system was constructed, which shows the area of possible separation of metallic iron droplets under ultra-reducing conditions (the shaded area is shown in fig. 5). To construct the diagram, diagrams of the state of the periclase-quartz, wustite-quartz and periclase-wustite systems at a pressure of 1 atm were used. The diagram of the state of the forsterite-fayalite system shows the stability region of metallic iron, the product of incongruent melting of ferruginous olivine at  $T = 1510^{\circ}\text{C}$ ,  $P = 1$  atm (Yoder, 1979). This makes it possible to approximate the area of compositions in which the metal phase Fe<sup>0</sup> can be formed in equilibrium with the melt and olivine crystals. The points of the experimental compositions marked with colored circles on the diagram fall into the region of melt, olivine crystals and the Fe<sup>0</sup> metal phase (red is

the initial composition; blue –  $1600^{\circ}\text{C}$ , 3 GPa; green –  $1600^{\circ}\text{C}$ , 2,5 GPa). As the pressure increased, the composition of the melt changed to the area of saturation of the system with silica, i.e. to the area of andesite composition.

In nature, there are deposits in the basalts of which there are quite large accumulations of iron, for example, Disco Island. According to E.M. Spiridonov are "Disco Island is a natural metallurgical process." The question of the origin of such deposits remains debatable. One of the points of view is the interaction of platiobasalts with the coal-bearing strata lying on metamorphites. Such iron accumulations could form at oxygen volatility close to the CCO buffer, but at low pressures.

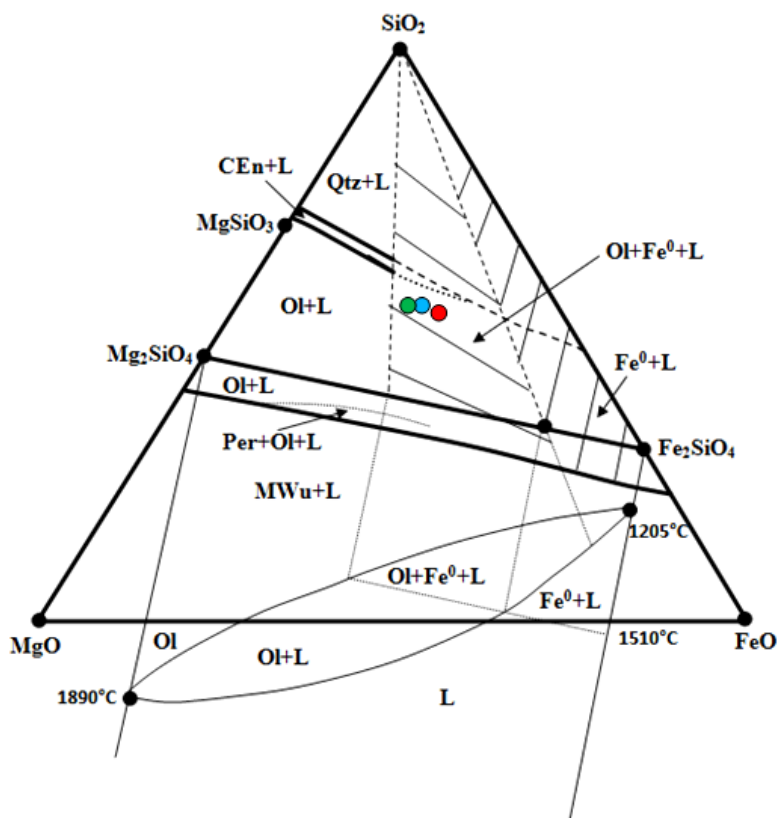


**Fig. 5.** The fusibility diagram for the  $\text{SiO}_2\text{-MgO-FeO}$  system, which shows the area of possible separation of the metallic phase of iron under reducing conditions. Melt compositions: red circle – initial composition; blue –  $T = 1600^\circ\text{C}$ ,  $P = 3$  GPa; green –  $T = 1600^\circ\text{C}$ ,  $P = 2,5$  GPa. Symbols: L – melt, Qtz – quartz ( $\text{SiO}_2$ ), Per – periclase ( $\text{MgO}$ ), Wu – wustite ( $\text{FeO}$ ), MWu – magnesio-wustite ( $(\text{Mg,Fe})\text{O}$ ), CEn – clinoenstatite ( $\text{MgSiO}_3$ ), Ol – olivine ( $\text{Mg}_2\text{SiO}_4$  (forsterite) –  $\text{Fe}_2\text{SiO}_4$  (fayalite)),  $\text{Fe}^0$  is metallic iron.

**Conclusions.** Experiments carried out on the "anvil with a hole" installation in an open system without platinum capsules do not allow to obtain metal droplets when buffering the system with carbon, because this area is at  $f\text{O}_2$  (CCO), which is higher than  $f\text{O}_2$  (IW). In the experiments of the  $\text{SiO}_2\text{-MgO-FeO-C-H}$  system, glasses saturated with calcium oxide were obtained at  $T = 1600^\circ\text{C}$  and  $P = 2,5\text{-}3$  GPa, the phase of calcium pyroxene crystallizes along the edges of the sample and graphite, in the form of inclusions, the central zone is represented by glass and quartz crystals, at  $T = 1500^\circ\text{C}$  and  $P = 3$  GPa, the glass structure becomes homogeneous and porous with large graphite inclusions. In the constructed diagram of the fusibility of the considered system, the composition points of the experimental samples fall into the stability region of the melt, olivine crystals and the  $\text{Fe}^0$  metal phase.

The work was carried out with the support of the state task of GEOKHI RAS.

### References

Bobrov A.V., Litvin Yu.A., Dymshits A.M. Experimental studies of carbonate-silicate systems of the mantle in connection with the problem of diamond formation // GEOS Moscow, 2011, 208 p.  
 Javoy M. The integral Enstatite Chondrite model of the Earth // Geophys. Res. Lett. 1995.V. 22. P. 2219-2222.

Kadik A.A., Kurovskaya N.A., Lukanin O.A., Ignatiev Yu.A., Koltashev V.V., Kryukova E.B., Plotnichenko V.G., Kononkova N.N. Formation of N-C-O-H molecules and complexes in basalt-andesite melts at 1.5 GPa and  $1400^\circ\text{C}$  in the presence of liquid iron alloys // Geochemistry, №2, 2017, pp. 115-126.  
 Kadik A.A., Litvin Yu.A., Koltashev V.V., Kryukova E.B., Plotnichenko V.G. Solubility of hydrogen and carbon in reducing magmas of the early mantle of the Earth // Geochemistry, № 1, 2006, pp. 38-53.  
 Lukanin O.A., Tsekhonya T.I., Koltashev V.V., Kononkova N.N. Influence of C-O-H volatile components on the distribution of Ni, Co and P between silicate melt and liquid metallic iron alloy at 4 GPa,  $1550^\circ\text{C}$  // Geochemistry, Volume 65, № 6, 2020, pp. 548-565.  
 McDonough W.F. Earth's core. Springer International Publishing. AG (2017). W.M. White (ed.), Encyclopedia of Geochemistry, p. 1-13.  
 Walter M.J., Newsom H.E., Ertel W., Holzheid A. Siderophile elements in the Earth and Moon: Metal/silicate partitioning and implications for core formation. In: Origin of the Earth and Moon / Eds. R.M. Canup, K. Righter. The University of Arizona Press, Tucson. 2000. P. 265-289.  
 Wanke H., Dreibus G. Chemistry and Accretion of Earth and Mars // LPC XV. 1984. P. 884-885.  
 Wetherill G.W. Formation of the Earth. // Ann. Rev. Earth Planet. Sci., 1990. V. 18. P. 205-256.  
 Yoder H. Formation of basalt magma. Moscow: Mir, 1979, 239 p.

**Shchekina T.I.<sup>1</sup>, Zinovieva N.G.<sup>1</sup>, Rusak A. A.<sup>2</sup>, Khvostikov V.A.<sup>3</sup>, Kotelnikov A. R.<sup>4</sup>,**

**Alferyeva Ya.O.<sup>1</sup>, Gramenitskiy E.N.<sup>1</sup>**  
**Crystallization of rock-forming minerals and rare elements phases in the fluorine enriched model granite system at a temperature reduction at a pressure of 1 kbar.**  
UDC: 552.11, 550.42

<sup>1</sup>Lomonosov Moscow State University, Department of Geology, Russia, 119991, Moscow, st. Leninskiye gory, 1, <sup>2</sup>Vernadsky Institute of Geochemistry and analytical chemistry RAS (GEOKHI RAS), Russia, 119991, Moscow, st. Kosygina, 19, <sup>3</sup>Institute of problems of technology of microelectronics and special-purity materials RAS (IPTM RAS), Russia, 142432, Chernogolovka, st. Institutskaya, 6, <sup>4</sup>Korzhiński Institute of Experimental Mineralogy RAS (IEM RAS), Russia, 142432, Chernogolovka, st. Institutskaya, 4 (t-shchekina@mail.ru, nzinov@mail.ru, aleks7975@yandex.ru, khvos@ipmt-hpm.ac.ru, kotelnik@iem.ac.ru, yanaalf@yandex.ru, engramen@geol.msu.ru).

**Abstract.** The process of phases crystallization in the model granite system Si-Al-Na-K-Li-F-O-H has a number of features with decreasing temperature. The main difference from granite systems without fluorine and lithium is the appearance of a salt phase in the liquidus part of the system, which is in equilibrium with the silicate melt, starting from a temperature of 800°C. Crystallization of alkaline aluminofluorides of K-Na cryolite composition begins at 750 - 700°C from the salt melt in the agpaitic part of the system and it continues up to 500°C. Starting from 600°C, quartz crystallizes from the silicate melt in the form of rounded grains together with K-Na aluminofluorides. They are often found inside quartz crystals, which indicates their simultaneous crystallization. At 600°C, alkali feldspar and Li-mica polyolithionite join them, forming wide rims at the contact of salt globules and silicate melt. Rare earth elements are concentrated mainly in the salt melt and are in the residual salt phases up to 600-500°C. When cooled, they form fluorides. The partition of petrogenic and rare earth elements between salt and aluminosilicate melts depends on temperature.

**Keywords:** *crystallization; aluminosilicate and aluminofluoride melts; residual salt melts; fluorine; lithium; rare earth elements; partition; temperature effect*

Previously, it was shown (Gramenitskiy et al., 2005) that in the agpaitic part of the Si-Al-Na-K-Li-F-O-H model granite system containing more than 3 wt.% fluorine and 1 wt.% lithium, at a temperature of 800°C phenomena of immiscibility arise between aluminosilicate (L) and alkaline aluminofluoride (salt LF) melts. Rare earth elements are concentrated mainly in the salt melt (Shchekina et al., 2020). Crystallization processes in such a system have a number of features compared to those occurring in a granite system not saturated with fluorine and lithium. The aim of the work was to study phase relations in the Si-Al-Na-K-Li-F-O-H system in the temperature range 1250-500°C from liquidus to solidus. The phases crystallization process as the granite system with the limiting fluorine content cools, as well as the behavior of rare earth elements and lithium in the system, have not been previously

studied in detail. The objectives of the study included: 1. Identification of the temperature and water content effect on the process of immiscibility between silicate and salt melts in the system during its cooling. 2. Establishment of the order of aluminosilicate, salt and rare earth phases crystallization and their composition when the temperature in the system decreases from 1250 to 500 °C at a pressure of P=1 kbar. 3. Study of the partition of petrogenic, rare earth elements and lithium between phases during system cooling.

**Technique and methods of experiment.** As the initial charge, a silicate-salt mixture of reagents was used: SiO<sub>2</sub>, NaF, LiF, AlF<sub>3</sub>, Al<sub>2</sub>O<sub>3</sub>, K<sub>2</sub>SiF<sub>6</sub>, corresponding to the granite eutectic composition, and the salt aluminofluoride component (Na,K,Li)<sub>3</sub>AlF<sub>6</sub> in a mass ratio of 1:1. The water content in the system varied from 3 to 50 wt.%, in most experiments it did not exceed 10-15 wt.%. The charge was introduced REE, Y, Sc in the form of oxides in the amount of 0.5-2 wt.% element, Li -1.5 wt.%. The experiments were carried out on a high gas pressure unit with internal heating at a temperature of 500-1250°C and a pressure of 1 kbar, a number of experiments were carried out at 700-800°C and at 1, 2, 3 and 5 kbar. The fugacity of oxygen in the experiments corresponded to that created by the NNO buffer. Experiments at 750 - 500°C were carried out as follows. The initial mixture was placed in platinum ampoules 3 mm in diameter, filled with a calculated amount of distilled water, the ampoules were brewed, placed in a reactor, and kept at a temperature of 800°C for 3 days. Then they were cooled for 8 hours to the desired temperature, kept for another three days and then hardened. The duration of the experiments was 7 days. Another method of achieving equilibrium was the approach to it "from below" at temperatures of 600 and 500°C and 1 kbar. The experiments were heated to a given temperature and kept for 7 days. In the charge of these experiments was introduced 10 or 20 wt.% water. To phases diagnose and determine their composition in relation to rock-forming elements, fluorine and oxygen, a Jeol JSM-6480LV scanning electron microscope (Jeol, Japan) with an Oxford X-MaxN energy-dispersive spectrometer (Oxford Instrument Ltd., Great Britain) was used.

The analysis of rare earth elements, yttrium, and scandium was carried out on a Superprobe JXA-8230 electron probe microanalyzer (Jeol, Japan) at the Laboratory of High Spatial Resolution Analytical Techniques, Department of Petrology and Volcanology, Faculty of Geology, Moscow State University. Mass spectrometry methods were used to determine the content of lithium in silicate and fluoride phases and rare earth elements in those phases where their concentration was very low.

Polished samples were studied using the laser ablation method at the Institute for Microelectronics Technology and High-Purity Materials of the Russian Academy of Sciences. The bulk composition of silicate, salt phases and fluid were studied by transferring the experimental material into solution on an Element-2 mass spectrometer of the Department of Geochemistry, Moscow State University.

**Results.** At the highest temperature of experiments 1250°C and water content from 0 to 10 wt.% in the liquidus part of the Si-Al-Na-K-Li-F-O-H system, aluminosilicate melt stably exists and at 10-32 wt.% H<sub>2</sub>O - melt and fluid. During quenching in the melt, heterogeneity is observed, associated with the appearance in the glass of small (less than 5 μm) rounded allocation of quenching fluoride phases. At 1000°C and water content from 0 to 5 wt.% in the system, the aluminosilicate melt L is also the only condensed phase. Starting with a water content of 10 wt.%, precipitates of a salt melt of LiKNa-aluminum fluoride composition (LF) appear in the aluminosilicate melt in the form of droplets forming

round or oval globules (Fig. 1a) up to 20 μm in diameter. Their composition differs in the ratio of Na, K, Li, sometimes F and Al, which suggests their non-equilibrium state. It is assumed that below 1000°C, when the system is saturated with water, signs of immiscibility of the silicate and salt melts appear. At 800°C in the system at all water contents from 2 to 50 wt.%, an equilibrium of aluminosilicate and salt melts is established (Fig. 1b). In this case, the equilibrium criteria were considered to be the large size of salt melt globules (more than 20 μm in diameter) and the composition constancy of both the silicate and salt phases, which were formed during quenching, respectively, by silicate glass and aggregates of small quenching crystals of aluminofluorides (LiKNaFP) and REE fluorides. Thus, there is a clear tendency to close the immiscibility region in the system between 1000 and 800°C, probably closer to 1000°C. When the temperature decreases to 750°C, the same phase relationships are maintained as at 800°C.

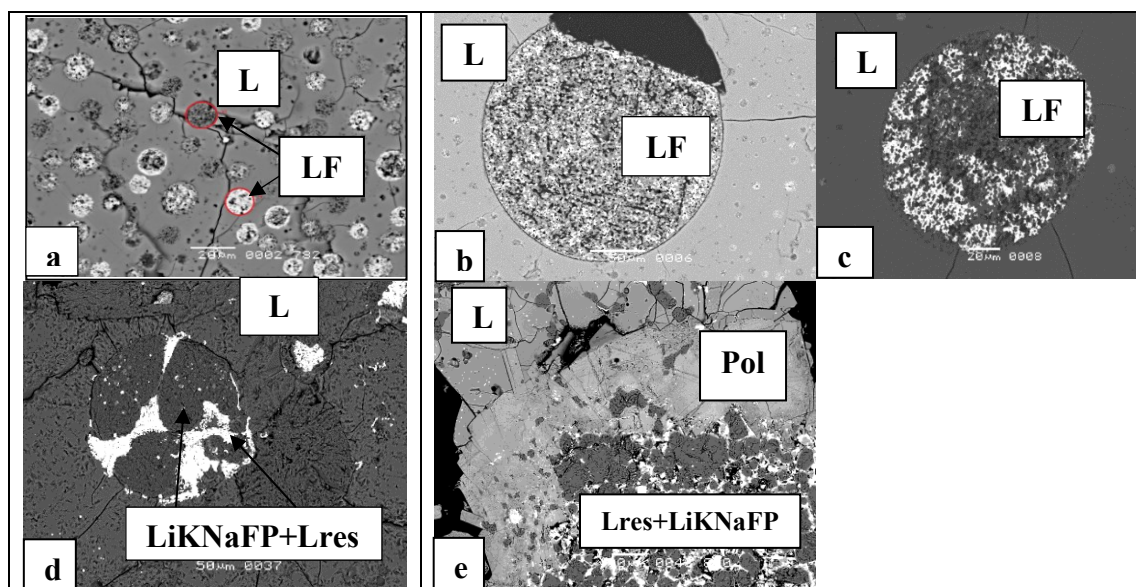


**Fig.1.** Phase relations in the Si-Al-Na-K-Li-F-O-H system at temperatures from 1000 to 500°C, 1 kbar: a -1000°C, b - 800°C, c - 750°C, d - 600°C; e - 500°C; f - 600°C approach "from below". Symbols: L-aluminosilicate melt; LF – aluminum fluoride salt melt; Lres – residual salt melt; LiKNaFP - aluminofluoride crystalline phase of cryolite stoichiometry; Pol - polyolithionite.

The difference is the formation of heterogeneity regions inside some salt melt globules (Fig. 1c): they show areas composed of an aggregate of quenching phases of aluminofluorides (LiKNaFP) and REE fluorides (light gray in BSE), and areas composed of quenching crystals of Na fluoride (dark gray in BSE) crystals that do not contain RER. At 700°C, the aluminosilicate melt is still in a liquid state, and the

salt melt begins to crystallize. Large crystals of LiKNa-aluminofluorides are formed in its globules (Fig. 1d), while some of the aluminofluorides have a essentially sodium composition, and some have a potassium-rich composition. The content of Li in them is 2-4 mass%. At 600°C, quartz begins to crystallize in the aluminosilicate melt. Close at the same time with quartz, Li-mica polyolithionite

crystallizes from the silicate melt at the boundary with salt globules (Fig. 1e). It often forms rims around globules up to 200 μm wide, but is found in glass and separately from salt globules. In the salt phase, Na- and K-aluminofluorides also continue to crystallize, containing also Li, but a residual salt melt rich in REE and Li remains. It surrounds aluminofluoride crystals (Fig. 1e) or penetrates between them. At 500°C, the system is not yet fully crystallized. Quartz continues to crystallize, forming large crystals with a typical faceting. Quite often, they contain segregations of LiKNa-aluminofluorides containing up to 5 wt.% Li. Part of the silicate and salt melts are in a supercooled, apparently metastable state, due to the high content of fluorine in the system. But new crystalline phases are no longer formed. Rare earth elements, remaining in the composition of the residual salt melt enriched with lithium, during crystallization form fluorides and alkaline fluorides containing small amounts of Na, K, and Li. The paper also considered phase equilibria in the system when approaching the equilibrium "from below". At a temperature of 500°C, 10 and 20 wt.% H<sub>2</sub>O, small crystals of quartz, KNa-feldspar, LiNaK-

aluminofluorides and rare earth fluorides are formed from the initial charge of reagents. At 600°C, 10 and 20 wt.% H<sub>2</sub>O, aluminosilicate glass and large crystals of the same minerals appear in the system (Fig. 1f).

**The discussion of the results.** The study of phase relations with a decrease in the temperature of the granite system made it possible to estimate the temperature of the beginning of melt separation into aluminosilicate and salt parts at about 1000°C and to investigate the phase crystallization sequence from liquidus to solidus. The features of the crystallization of the system were found, namely, that the salt melt begins to crystallize first, and then the silicate one. The boundaries of the silicate and salt phases in the system remain clear. An important observation was the discovery in the salt phase of a residual melt saturated with rare earth elements, which is in a liquid state up to 500°C. REE concentrations reach over 10 wt%. The partition coefficients between the aluminofluoride (FP) and silicate (L) phases of rock-forming elements manifest themselves differently depending on the temperature of the experiment (Fig. 2).

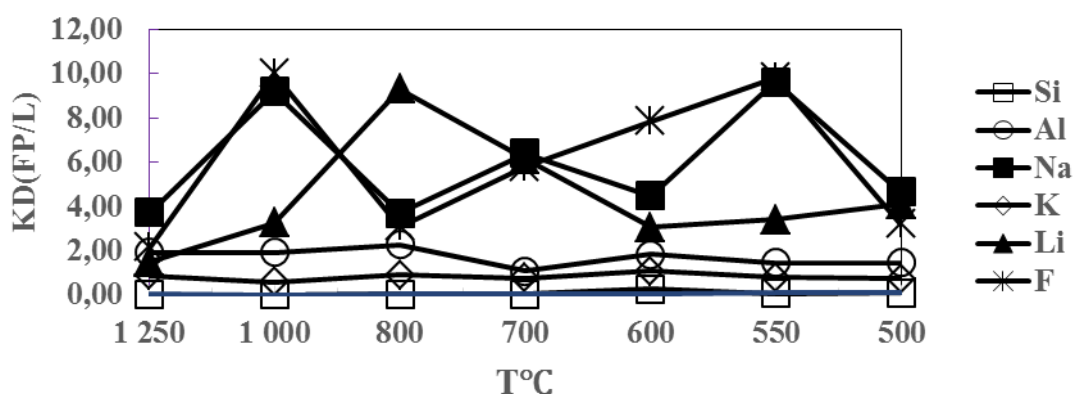


Fig.2. Dependence of coefficient KD(FP/L) of partition of Si, Al, Na, K, Li and F on temperature. Note: L is an aluminosilicate melt, FP is a fluoride melt, with a possible partial capture of other phases of the globule in the analysis of Li by the La-ablation method.

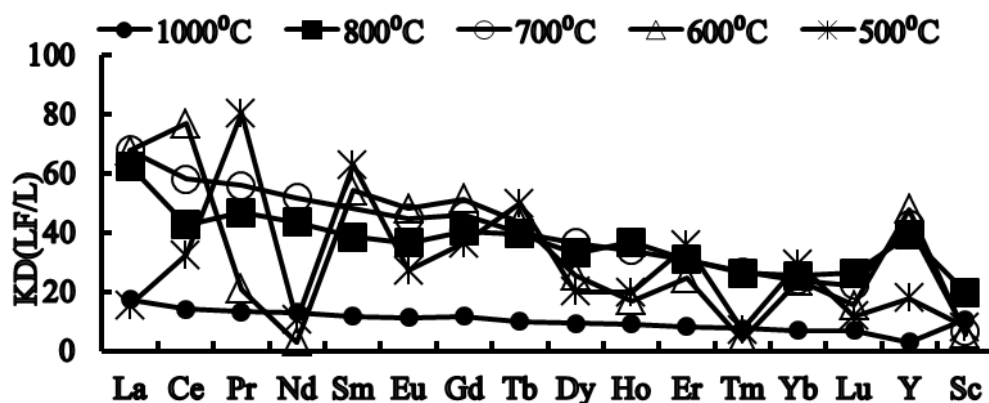


Fig. 3. Relationship of partition coefficients KD(LF/L) with temperature.

The KD (FP/L) of silicon is always low because Si practically not dissolving in the salt melt; for potassium, it is low, close to 1, and practically constant at all temperatures. KD (FP/L) of Na, Li and F are usually significantly greater than 2, since they are predominantly distributed in favor of the salt phase. At some temperatures, there is a direct relationship between the partition coefficients of Na and c F or Na and Li with F. The variability of the behavior and relationships of the elements with each other is complicated by the crystallization of the phases when the system is cooled. The KD (FP/L) of Li is maximum at 800°C, presumably because at this temperature the salt phase is homogeneous, not including any Li-containing phases other than the melt. It can be concluded, considering Fig. 2, that the partition factors are influenced by phase relations in the system.

The nature of the spectra of partition coefficients of rare earth elements between aluminosilicate and salt melts is related to temperature. At 1000-800-700°C under conditions of coexistence of 2 melts, KD(LF/L) will gradually decrease from light to heavy REE.

As the temperature decreases and the system crystallizes, sharp deviations appear in the course of the KD(LF/L) spectra for some elements (Nd, Tm), sometimes associated with the impossibility of obtaining a representative analysis of inhomogeneous regions of the residual salt melt.

**Conclusion.** 1. The region of immiscibility in the Si-Al-Na-K-Ki-Li-F-O-H system between the aluminosilicate and salt melts closes at a temperature of ~ 1000 °C at 1 kbar and a water concentration of ~10 wt.%. 2. Crystallization of the system begins at 700 °C in a salt melt with the appearance of Na-aluminum fluoride, which is close to cryolite. Such cryolite segregations are characteristic of cryolite-bearing granites and form deposits. 3. Crystallization of the silicate melt begins in the temperature range between 700 and 600°C from quartz, to which Li-mica and KNa-aluminofluorides are added. The melt remains in the system up to 500°C. Its composition is close to that of the eutectics of F-bearing granite. 4. REE, Y, Sc accumulates in the residual salt melt with decreasing temperature, showing off itself as incompatible elements with a high affinity for fluorine and lithium. Rare earth elements accumulated in residual melts can be a source for the formation of corresponding deposits.

---

Sources of funding: state task of GEOKHI RAS, RFBR (project № 16-05-0089). During the research, equipment purchased at the expense of the Moscow University Development Program was used.

---

## References

- Gramenitsky E.N., Shchekina T.I., Devyatova V.N. Phase relations in fluorine-containing granite and nepheline-syenite systems and distribution of elements between phases. M.: GEOS – 2005. – 186 p.
- Shchekina T. I. Rusak, A. A., Alferyeva Ya. O., Gramenitskiy E. N., Kotelnikov A. R., Zinovieva N. G., Bychkov A. Yu., Bychkova Ya. V., and Khvostikov V. A. REE, Y, Sc, and Li Partition between Aluminosilicate and Aluminofluoride Melts, Depending on Pressure and Water Content in the Model Granite System. *Geochemistry International*. –2020. Vol. 58, № 4. –P. 391–407.